Journal of the Korean Electrochemical Society
Vol. 11, No. 1, 2008, 37-41

Electrochemical Properties and Structural Analysis of Carbon-Coated Silicon Anode for Lithium Secondary Batteries

Hyung Sun Kim*, Kyung Yoon Chung, and Byung Won Cho

Battery Research Center, Korea Institute of Science and Technology, Seoul 136-791, South Korea

(Received January 28, 2008 : Accepted February 5, 2008)

Abstract : The effects of carbon-coated silicon anode on the electrochemical properties and structural change were investigated. The carbon-coated silicon powders have been prepared by thermal decomposition under argon/10wt% propylene mixed gas flow at 700°C. The surface and crystal structure of the synthesized materials were examined by scanning electron microscopy (SEM), transmission electron microscopy (TEM), and Raman spectroscopy. Lithium cells with electrodes made from the uncoated and the carbon coated silicon anode were assembled and tested. The carbon-coated silicon particles merged together well after the insertion/extraction of lithium ions, and showed a relatively low irreversible capacity compared with the uncoated silicon particle.

Keywords : Lithium secondary battery, Carbon-coated silicon anode

1. Introduction

There has been considerable interest in the silicon active material as a promising anode for lithium ion batteries. This material offers a very large lithium insertion capacity of 4200 $mAhg^{-1}$. In addition, the potential of lithium insertion into silicon is < 0.5 V vs. Li/Li^+, which is suitable as an anode material.[1] However, the large volumetric change during lithium insertion/extraction cycling and the intrinsic low electrical conductivity of silicon are shortcomings when using silicon. These factors result in poor cycling performance and low lithium uptake at high current density. Many attempts have been made to solve these problems by coating the silicon particle surface with a conducting material.[2-6] Among these techniques, a carbon-coating method has been used widely to improve the electrical conductivity of nanosized silicon particles. These developed systems have shown reversible capacity as high as 1000 $mAhg^{-1}$.[7] Although this technology has improved the electrochemical performance of silicon, the structural changes needs to be studied during the formation of an alloy/de-alloy phase with lithium insertion/extraction. Research on these structural changes is very important for developing a silicon anode. The crystal structural evolution of the silicon anode has been studied in more detail using Raman spectroscopy.[8] It was found that the insertion of lithium ions gradually destroys the crystal structure of silicon, which leads to the formation of a metastable amorphous Li-Si alloy.

In this paper, a carbon-coated silicon anode was prepared by hydrocarbon gas decomposition and its effect on the structural changes and electrochemical performances was compared with that of an uncoated silicon anode.

*E-mail: kmhs@kist.re.kr

2. Experimental

Commercial microcrystalline nanosized silicon powder (Alfa Aesar, 98%) was used as the starting material. The silicon powder was batched at a tubular furnace and decomposed thermally at 700°C for 7 h under argon containing 10wt% propylene gas to form a carbon phase on the surface of the powder. The crystal structure of the powders was analyzed by dispersive Raman spectroscopy (Nicolet Almega XR, Thermo Electron Corp.). The morphology of the electrodes was examined by transmission electron microscopy (TEM, Philips CM 30) and scanning electron microscopy (SEM, Hitachi 4200).

The electrode was prepared by mixing the obtained silicon powders (50wt%) with poly(vinylidene fluoride) binder solution (30wt%), acetylene black conductive material (20wt%) and N-methyl pyrrolidinone (NMP) organic solvent in a high speed mixer. The mixed viscous slurry was cast onto copper foil current collectors using the doctor blade technique and dried at 80°C in a vacuum oven for 24 h. The resulting electrode was used as the working electrode in a cell with a lithium metal counter electrode. The electrolyte used was 1M $LiPF_6$ in a mixture of ethylene carbonate (EC), dimethyl carbonate (DMC) and ethyl-methyl carbonate (EMC) (1 : 1 : 1 in vol%, Cheil Industries Inc., South Korea). The separator was a Celgard 2400 microporous polypropylene membrane. All cells were enveloped in aluminum plastic pouches and sealed under vacuum in a dry room (dew point: −50°C). The impedance spectra of the assembled cells were recorded by impedance gain phase analyzer (Solartron SI 1260) coupled with electrochemical interface (Solartron SI 1286). The cells were cycled using galvanostatic and cyclic voltammetry methods over the potential range of 0.005 and 1.0 V using a Maccor

battery cycler (S 4000, USA).

3. Results and discussion

Fig. 1 shows the Raman spectrum of the carbon-coated silicon powder and uncoated silicon powder, respectively. This spectrum was recorded with a 633.0 nm excitation line. The sharp peak centered at approximately 520 cm^{-1} corresponds to the typical crystalline silicon phase, while the two broad peaks at 1350 cm^{-1} and 1590 cm^{-1} are related to the carbon phase. In the spectrum of a pure carbon film, the position of the D (amorphous carbon) and G (graphitic carbon) bands was 1340 cm^{-1} and 1582 cm^{-1}. These bands also correspond to the sp^3 (disordered carbon) and sp^2 (graphite) carbon stretching modes, respectively. The positions and relative intensities of the G and D bands provide more information on the structure and domain size of a carbon material.[9] The two wide, broad peaks indicate that the carbon layer is composed of crystalline graphitic and amorphous carbon. This result also was confirmed by TEM image presented in Fig. 6.

Fig. 2(A-C) shows that the impedance spectrum results of Li/Si half cell at various states. Impedance spectroscopy measurements were performed over a frequency range from 1 MHz to 0.1 Hz. The ac amplitude used during the measurement was 10 mV. Fig. 2(A) shows almost similar resistance value at the initial state irrespective of carbon coating. At high frequency, the line intercepts the real part and this point corresponds to the resistance of electrolyte (R_b). This value increased slightly after charge and discharge due to the decomposition of electrolyte. When the cell is discharged to 5 mV vs. Li/Li^+ at constant current density of 0.25 $mAcm^{-2}$, the carbon-coated Si anode shows lower resistance than that of uncoated Si anode as shown in Fig. 2(B). The first semi-circle (Rc) at high frequency represents the inter-particle contact resistance.[10,11] Therefore, the reduction in the diameter of the semi-circle may be attributed to the decreased contact resistance by carbon coating. This contact resistance also increased when the cell was charged to 1.0 V vs. Li/Li^+ as shown in Fig. 2(C). The second semi-circles (Rp) at low frequency increased significantly after discharge and charge test, respectively. This phenomenon can be ascribed to a growth of a passive layer thickness due to the reactivity of the electrode and electrolyte. No straight line was obtained in the low frequency region, which represents a diffusion-controlled process in the solid electrode. Therefore, we believe that the insertion and de-insertion reaction of lithium into composite electrode is mainly dominated by the interfacial resistance between electrolyte and electrode. Fig. 3 shows the cyclic voltammograms obtained for the first five cycles of the carbon-coated silicon and the uncoated silicon anode, respectively. Both electrodes had a uniform sample size (2 cm × 2 cm) and the same amount of active material (1.6 $mgcm^{-2}$). In the first sweep cycle of both electrodes, the

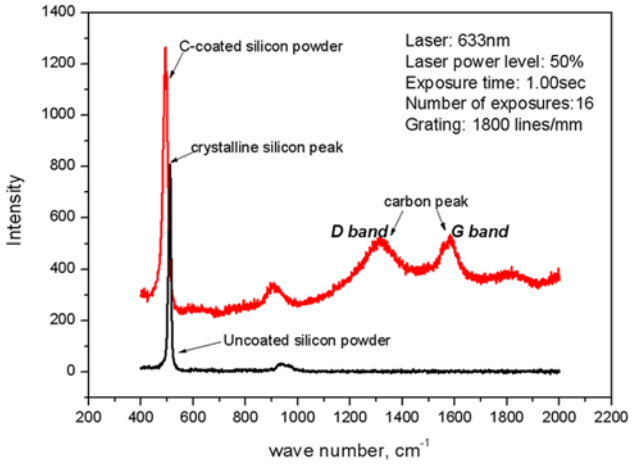

Fig. 1. Dispersive Raman spectrum of the c-coated Si and uncoated Si particles.

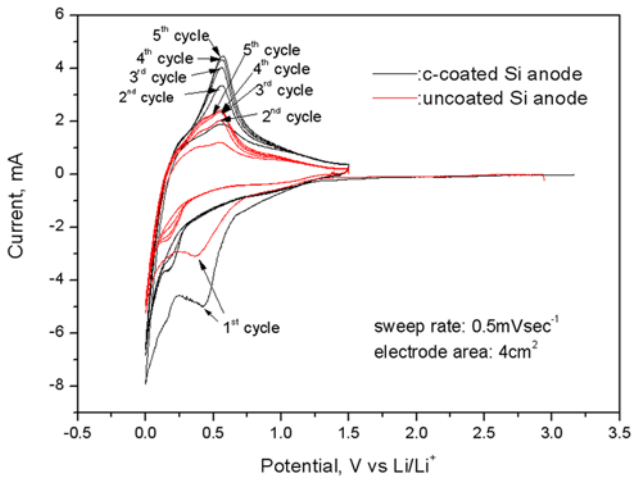

Fig. 3 Cyclic voltammograms of the Li/Si cells at room temperature.

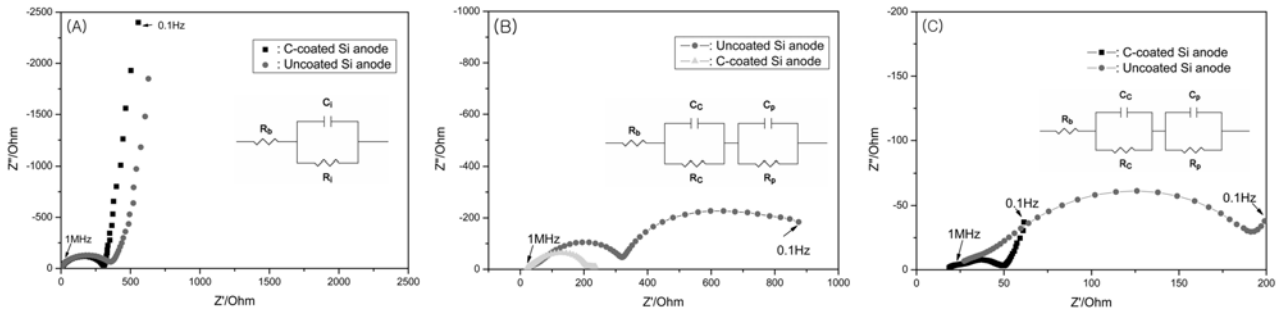

Fig. 2. AC impedance spectrum of Li/Si cells at various states (A: initial state, B: discharged state, C: charged state).

irreversible cathodic current increased sharply <0.7 V vs. Li/Li^+, which is related to the formation of a solid electrolyte interphase and a side reaction between the electrode and electrolyte. A reversible cathodic current (Li alloying) then flows below 0.25 V vs. Li/Li^+, which is related to the transformation of silicon from a crystalline phase to an amorphous phase.[12] From the second cycle, the irreversible cathodic current peaks disappeared and the increased anodic peak currents (Li de-alloying) were observed at both electrodes. Once the SEI interface forms, a new SEI layer does not form under subsequent reaction of Li alloying and Li de-alloying. So, it can be considered that the increased anodic current peaks may be attributed to the reduced side reaction as cycle proceeds. The reversible anodic current increased sharply to 4.2 mA in the carbon coated silicon anode, and 2.3 mA in the uncoated silicon anode. This indicates that the carbon coated silicon anode can offer better conductivity than the uncoated silicon anode by decreasing the contact resistance between active materials. Fig. 4 shows the result of a comparative charge/discharge curves for the carbon coated silicon

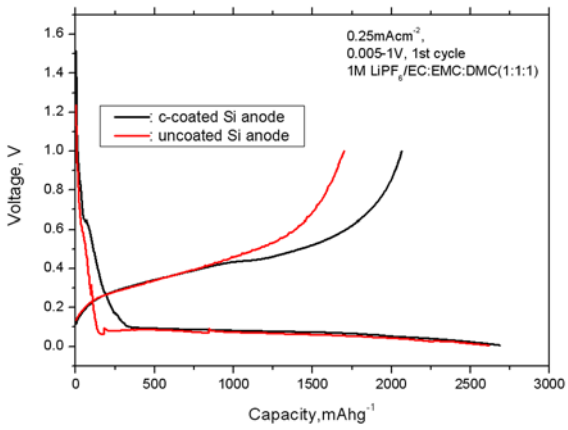

Fig. 4. Charge/discharge curves of the Li/Si cells at the first cycle.

Table 1. Discharge/charge capacity vs. cycle number of carbon-coated silicon anode and uncoated silicon anode for the first five cycles

Cycle Number	carbon coated Si anode (discharge capacity/charge capacity, mAh/g)	uncoated Si anode (discharge capacity/charge capacity, mAh/g)
1st	2700 / 2250	2700 / 1750
2nd	2320 / 2170	1840 / 1400
3rd	2240 / 2100	1490 / 1300
4th	2150 / 2000	1340 / 1220
5th	1960 / 1810	1240 / 1140

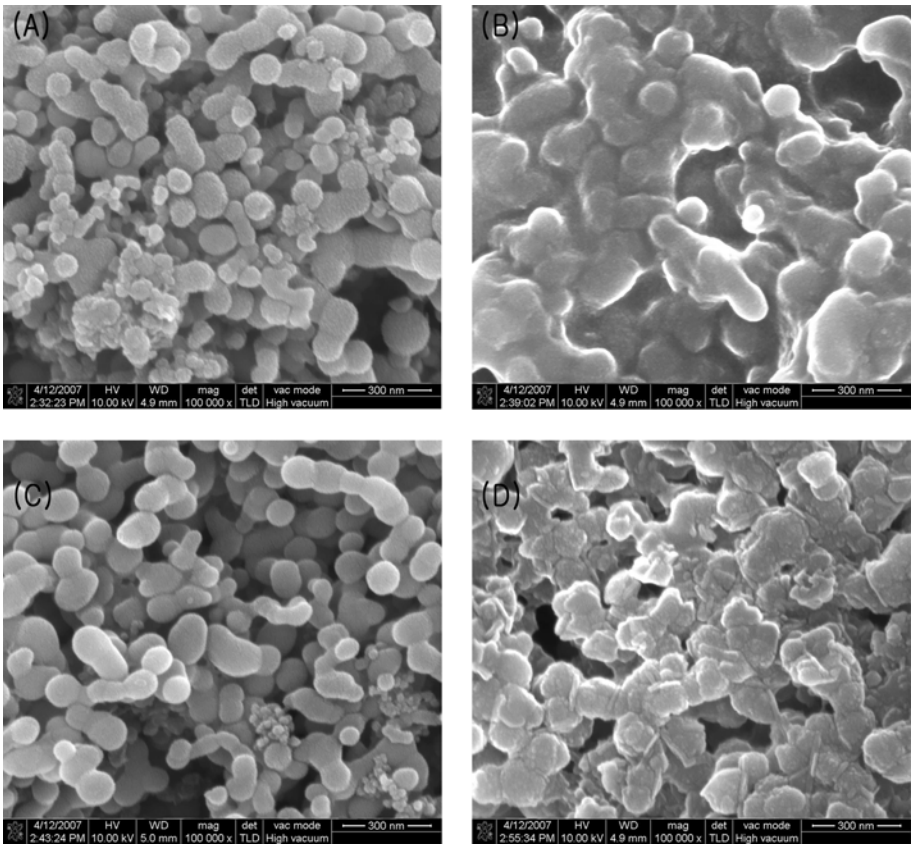

Fig. 5. SEM images of various Si anodes (A: c-coated Si anode before cycling, B: c-coated Si anode after the 5th cycle, C: uncoated Si anode before cycling, D: uncoated Si anode after the 5th cycle).

first discharge capacity of both electrodes was 2700 $mAhg^{-1}$, while the charge capacity of the carbon coated and uncoated silicon anode was 2250 $mAhg^{-1}$ and 1750 $mAhg^{-1}$, respectively. As shown in Fig. 4, the carbon coated silicon anode showed a more stable electrochemical performance with high coulombic efficiency $>80\%$ due to the full lithium insertion/desertion reaction into the silicon powders.

Discharge/charge capacity of carbon coated silicon anode and uncoated silicon anode for the initial five cycles are summarized in Table 1.

The SEM morphology was observed after the 5th cycle in order to further understand the reason for the improved coulombic efficiency of the carbon-coated silicon anode. Fig. 5(A-D) shows the surface structures of the carbon-coated anodes and the uncoated anodes before and after the 5th cycling test. It was found that many dispersed silicon particles had coalesced after the cycling test. When compared with Fig. 5(B) and Fig. 5(D), silicon reacts with lithium well after the carbon coating. The TEM results in Fig. 6 suggest that the structural variation in the carbon-coated anode fully changed from a crystalline to an amorphous phase. These amorphous regions can be regarded as the part that reacted with lithium. This structural change results in the detachment of the active material from the copper current collector, and electrode loses its electrical contact with the substrate. Therefore, the cycling performance of the carbon-coated silicon anode cannot be improved substantially without solving this problem. It was reported that a silicon anode pasted on a nickel foam current collector showed stable cyclic performance with high capacity.[13] This three-dimensional electrode configuration might preserve the stable electrochemical property despite the microstructural changes in the active materials. Fig. 7 shows TEM images of the uncoated silicon anode before and after the 5th cycling test. Unlike the carbon-coated silicon anode, the structural variation in the uncoated anode partly changed from a crystalline to amorphous phase. The crystalline phase part of the silicon core and the amorphous regions of the silicon outer are clearly distinguished from the image presented in Fig. 6. This result also supports the reason that the carbon coating method enhances the utilization of the silicon active material.

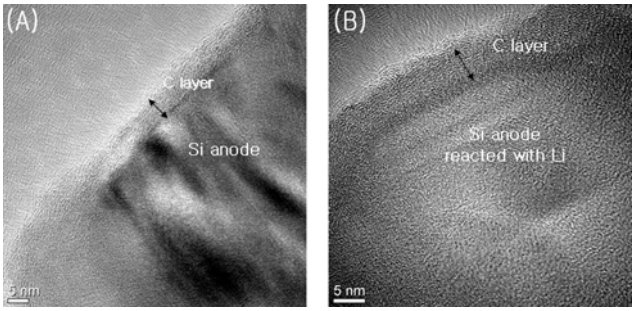

Fig. 6. TEM images of c-coated Si anodes before cycling (A) and after the 5th cycle (B).

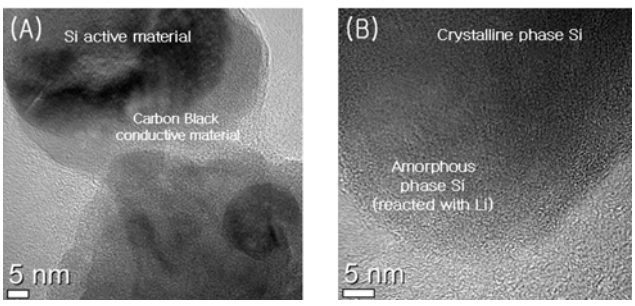

Fig. 7. TEM images of the uncoated Si anodes before cycling (A) and after the 5th cycle (B).

4. Conclusions

These results show that microcrystalline nanosized silicon powder can be used as high capacity anode material for lithium secondary batteries. The carbon-coated silicon anode showed better coulombic efficiency than the uncoated silicon anode. However, the structural change was much more severe due to the higher utilization of the silicon active material. This results in the detachment of the active material from the copper current collector. Although the carbon coating is an effective method to improve the electrical conductivity of the silicon powder, this might be not enough to improve the long-term cycling performance. Therefore, further studies on amorphous silicon alloys as well as a 3-dimensional frame current collector will be needed to overcome these problems in the future.

Acknowledgements

This work was carried out with the financial support from the Core Technology Development Program of the Ministry of Commerce, Industry and Energy.

References

1. N. Dimov, S. Kugio and M. Yoshio, Carbon-coated silicon as anode material for lithium ion batteries, Electrochimica Acta, **48**, 1579 (2003).
2. X. Wu, Z. Wang, L. Chen and X. Huang, Ag-enhanced SEI formation on Si particles for lithium batteries, Electrochemistry Communications, **5**, 935 (2003).
3. W. Xing, A.M. Wilson, G. Zank and J.R. Dahn, Pyrolysed pitch-polysilane blends for use as anode materials in lithium ion batteries, Solid State Ionics, **93**, 239 (1997).
4. J. Shu, H. Li, R. Yang, Y. Shi and X. Huang, Cage-like carbon nanotubes/Si composite as anode material for lithium ion batteries, Electrochemistry Communications, **8**, 51 (2006).
5. H. Lee, Y. Kim and S. Lee, Graphite-FeSi alloy composites as anode materials for rechargeable lithium batteries, J. Power Sources, **112**, 649 (2002).
6. N. Dimov, K. Fukuda, T. Umeno, S. Kugino, M. Yoshio, Characterization of carbon-coated silicon Structural evolution and possible limitations, J. Power Sources, **114**, 88 (2003).
7. H. Lee and S. Lee, Carbon-coated nano-Si dispersed oxides/graphite composites as anode material for lithium ion batteries, Electrochemistry Communications, **6**, 465 (2004).
8. H. Li, X. Huang, L. Chen, G. Zhou, Z. Zhang, D. Yu, Y. Mo and N. Pei, The crystal structural evolution of nano-Si caused by lithium insertion and extraction at room temperature, Solid State Ionics, **135**,

181 (2000).
9. Z. Zhang, C. Dewan, S. Kothari, S. Mitra and D. Teeters, Carbon nanotube synthesis, characteristics, and microbattery applications, Materials Science and Engineering B **116**, 363 (2005).
10. Z. P. Guo, J. Z. Wang, H. K. Liu and S. X. Dou, Study of silicon/ polypyrrole composite as anode materials for Li-ion batteries, J. Power Sources, **146**, 448(2005).
11. W. Liu, Z. Guo, W. Young, D. Shieh, H. Wu, M. Yang and N. Wu, Effect of electrode structure on performance of Si anode in Li-ion batteries: Si particle size and conductive additive, J. Power Sources, **140**, 139 (2005).
12. T. Jiang, S. Zhang, X. Qiu, W. Zhu and L. Chen, Preparation and characterization of silicon-based three-dimensional cellular anode for lithium ion battery, Electrochemistry Communications, **9**, 930 (2007).
13. M. Yoshio, T. Tsumura and N. Dimov, Electrochemical behaviors of silicon based anode material, J. Power Sources, **146**, 10 (2005).